Ain Shams University, Enginerring Bulletim
Vol. 25, No. 3, Dec., 1990, Page 157-181

EXPERIMENTAL STUDY OF THE HYDRAULIC JUMP OVER ROUGH BEDS

Sharl S. Sakla[1], Mohamed A. El-Samanoudy[2], Mahmoud M. El-Gamal[3], and Amro M. El-Feki[4]

1 Prof. and Head of Irri. and Hydr. Dept., El-Mansoura Univ.
2 Assoc. Prof., Dept. of Irri. and Hydr., Ain Shams Univ.
3 Lecturer, Irri. and Hydr. Dept., El-Mansoura Univ.
4 Assist. Lecturer Irri. and Hydr. Dept., El-Mansoura Univ.

ABSTRACT

This paper concerns the determination of the hydraulic jump properties over rough impervious beds. An extensive experimental study of the hydraulic jump occurring on smooth and rough test beds are carried out.

Course sand and gravel of different sizes are used to prepare the various test beds for the experimental investigation. Different methods for describing the measure of bed roughness are included in this investigation. Free hydraulic jumps are formed in a rectangular flume downstream weir models of different geometrical scale ratios to obtain various inlet flow conditions. The experiments are carried out with different rates of discharge to cover wide range of Froude number. The experimental results of the properties of hydraulic jump for various flow conditions and different bed roughnesses are graphically presented in this paper. A useful empirical relation is deduced to give the ratio of the jump length over a rough bed to the corresponding length over a smooth bed as a function of the relative roughness height.

1. INTRODUCTION

The experimental determination of the physical parameters of the hydraulic jumps occurring over rough beds would be useful. They may also be used to formulate the necessary relations characterizing the hydraulic jumps occurring over rough beds. From the practical point of view the results of this study would be useful for the design of the hydraulic jump type stilling basins with a horizontal floor. Proper stilling basins should ensure the following requirements: high energy dissipation, necessity of low tailwater level, compactness and economical design of structure, stability of the process under variable discharges, and safety against cavitation erosion.

These requirements are usually met by installing certain accessories such as chute blocks, baffle piers and end sills along the basin floor. Alternatively, this may also be achieved by the installation of rough floor stilling basins.

The concrete floor can be roughened by installing large gravels, stones or concrete blocks during the construction and should be placed as closely as possible to produce rough floor stilling basin. The results and relations obtained from this investigation should aid in the design of stilling basins with rough floor.

The experiments of the hydraulic jump on rough bed were performed in a closed circuit laboratory flume. The supercritical flow was produced by weir models with different heights. The downstream water depth was controlled by the flume tail gate at the downstream end of the flume. Five types of bed roughnesses were studied. These roughnesses were produced by sticking gravel of different sizes to the floor steel plates by means of the epoxy glue substance.

The problem was first approached by the dimensional analysis of the hydraulic jump over rough bed to have the advantages of deducing the dimensionless parameters representing the governing factors of this problem.

2. Dimensional Analysis

Experimental programs require correlation between the gathering of data and its graphical representation. Before experimental results can be utilized, it is necessary to ascertain the functional form of the quantities entering the jump relations. In order to achieve this aim the dimensional analysis approach is applied to the present problem.

At first, it is important to identify the important physical quantities involved. Consider the simple two-dimensional model of hydraulic jump formed on rough bed, as illustrated in Fig. 1.

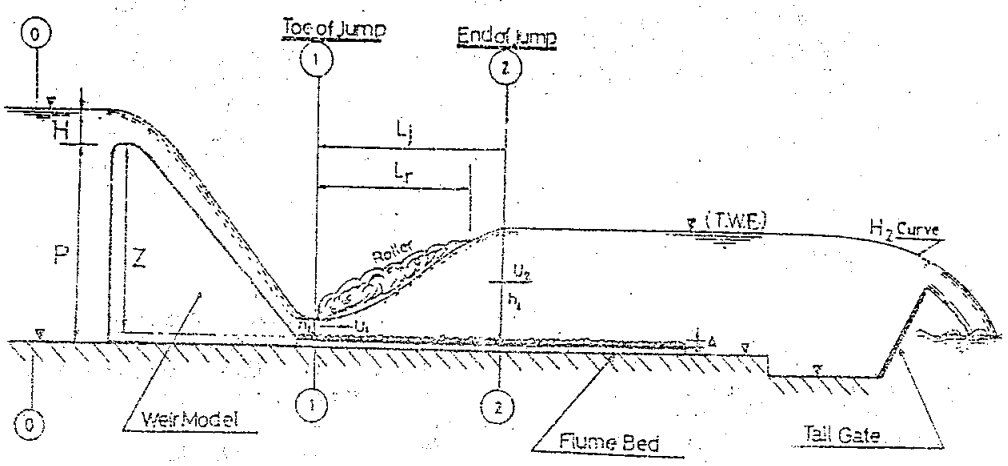

Fig. (1) Definition Sketch of The Flow Pattern Downstream Weir Model.

In the present study, the independent variables considered in the dimensional analysis are chosen to represent the experimental conditions of the problem. The following are the parameters considered for the dimensional analysis:

Z = drop height of weir model;
Δ = height of roughness elements;

W = width of flume;
h_1= hydraulic jump initial depth;
h_2= hydraulic jump sequent depth;
L_j= Length of jump;
q = discharge per unit width of flume;
g = acceleration due to gravity;
ρ = mass density of fluid; and
μ = dynamic viscosity.

2.1 The Determination of a Non-dimensional Relationship for The Length of The Hydraulic Jump over Rough Bed

The above mentioned variables are employed in the following dimensional analysis to obtain a relationship for the length of a free jump over a rough bed. The length of the jump may be expressed as an arbitrary function f_1 of the physical parameters of the problem to be in the form :

$$L_j = f_1(h_1, h_2, q, Z, W, \mu, g, \rho, \Delta) \quad (1)$$

The homogeneous function of the relation 1 may be written as ;

$$f_2(L_j, h_1, h_2, q, Z, W, \mu, g, \rho, \Delta) = 0 \quad (2)$$

in which f_2= another arbitrary function.

It is seen that L_j is dependent on nine independent variables having three dimensional units, hence seven independent dimensionless groups can be formed, using Buckingham's Pi Theorem. The relation 2 can be arranged and written in the following functional form,

$$\frac{L_j}{h_1} = f_4 \left(\frac{h_2}{h_1}, \frac{Z}{h_1}, \frac{W}{h_1}, \frac{\Delta}{h_1}, F_1, R_e \right) ; \quad (3)$$

in which, R_e = the Reynolds number.

The dimensional considerations show that the dimensionless jump length also depends on Reynolds number R_e. However for large values of R_e, the effect of fluid viscosity on turbulent diffusion is small. Thus neglecting the Reynolds number, Eq. 3 becomes :

$$\frac{L_j}{h_1} = f_5 \left(\frac{h_2}{h_1}, \frac{Z}{h_1}, \frac{W}{h_1}, \frac{\Delta}{h_1}, F_1 \right); \quad (4)$$

2.2 The Dimensionless Relation for The Conjugate Depth Ratio of Hydraulic Jump over Rough Bed

The conjugate depth of the jump could be written as :

$$h_2 = f_6 (h_1, L_j, q, Z, W, \mu, g, \rho, \Delta); \quad (5)$$

Similarly, from Buckingham's Pi theorem, the following dimensionless relationship for the conjugate depth ratio is obtained,

$$\frac{h_2}{h_1} = f_7 \left(\frac{L_j}{h_1}, \frac{Z}{h_1}, \frac{W}{h_1}, \frac{\Delta}{h_1}, F_1 \right); \quad (6)$$

3. Experimental Apparatus

The experiments are conducted in a laboratory flume. The flume, which is of the re-circulating type, has parallel steel sides and a rectangular cross section of 61 cm width, 20 cm depth and of 4.0 ms length.

The apparatus was inadequate for carrying out the experiments. The depth of the flume was not sufficient to contain the water depth for this investigation in the approach channel Therefore additional steel parts to extend the sides of the approach channel were made and then mounted to the sides of the apparatus After this modification the depth of approach channel is 60 cm. The purpose of this modification is to enable the placing of a number of weir models with different heights at the end of the approach channel in order to create a supercritical flow at the foot of the weir model. The supercritical flow would be changed to a subcritical flow by the formation of the hydraulic jump.

The maximum discharge of the pump operating the original flume was 11 lit/sec. Such a discharge is not sufficient to enable this investigation to have wide range of results. Therefore a new pump of a maximum discharge of 20 lit/sec is installed to replace the rig original pump.

The channel was originally supported on a steel tank at each end. In view of the increased weight of water stored upstream of the weir model and to ensure the strength and stability of the channel, two steel stands are made to support the flume at the middle.

The shape and main dimensions of the flume after these modifications are shown in Fig. 2.

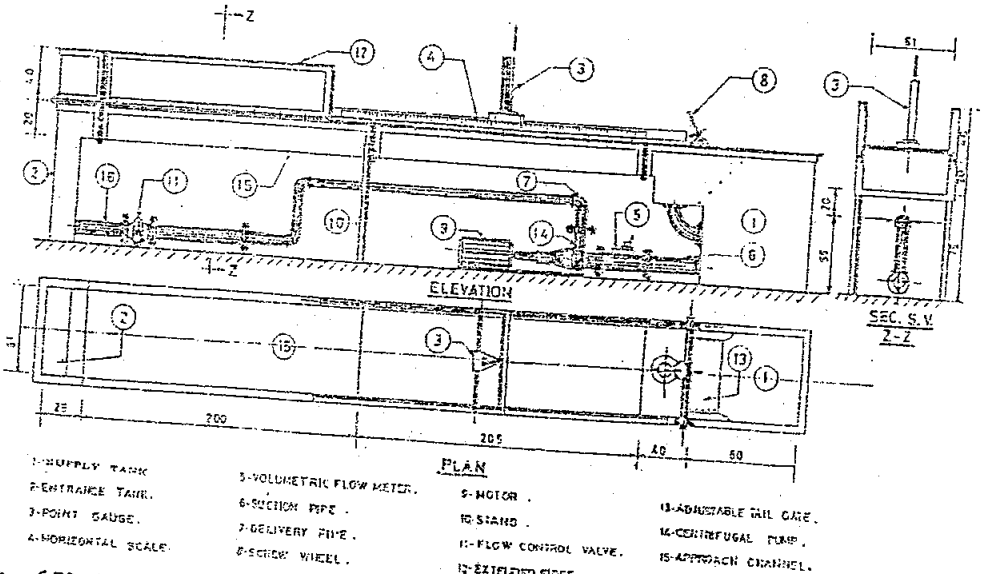

Fig. (2) The Experimental Flume Used for The Investigation.

The downstream depth is adjusted by means of an inclined gate located at the end of the flume as shown in Fig. 2. A hand driven gear system is used for the lifting or lowering of the tail gate, to change the downstream water depth.

4. The Weir Models

The present experimental investigation is carried out using four weir models with different dimensions. The main dimensions of the four models are summarized in Table 1.

TABLE (1) DIMENSIONS OF THE FOUR WEIR MODELS

MODEL NO.	SIZE	DROP HEIGHT Z_{th}, cm	MODEL HEIGHT P, cm	CREST WIDTH δ_o, cm	BASE WIDTH B, cm	CREST LENGTH W, cm	HEIGHT OF SIDE WALL cm	ACTUAL DROP HEIGHT Z, cm
1	Small	10	11	2	12	60.5	60	11.0
2	Medium	20	21	4	24	60.5	60	22.3
3	Large	30	31	6	36	60.5	60	32.5
4	V.Large	40	41	8	48	60.5	60	43.0

The definition sketch of the above mentioned dimensions is given in Fig. 3.

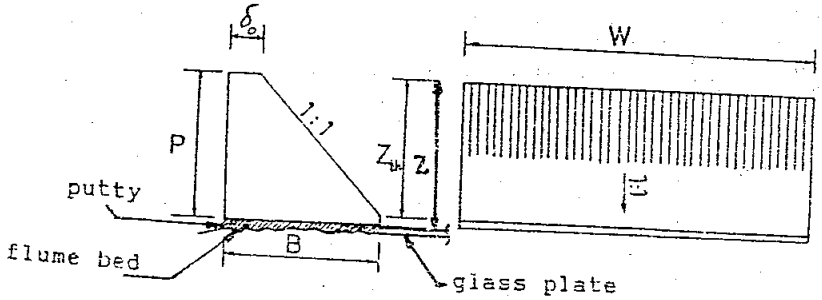

Fig. (3) Definition Sketch for The Dimensions of The Weir Model.

It is shown in Table 1 that the models No. 1, 2 and 4 are three geometrically similar models with geometrical scale progressing by the factor of two. The drop height Z_{th} was used as a characteristic linear dimension to compare one model with the other. Also, the models No. 1 and 3 are two geometrically similar models with the scale ratio of three. For each experiment, one weir model is fitted into the end of the approach channel. Putty was used to fill the narrow gapes, in order to prevent any leakage at the sides and the bed of the weir models.

The weir height is changed when the weir is fitted with the channel bed as a result of the levelling of the bed with putty to overcome its previous irregularity. The actual drop heights are measured for each weir model and are given in Table 1.

5. The Preparation of Test Beds

Artificially roughened test beds are prepared for the present investigation. This is carried out by the coating of rectangular steel plates, of the dimensions 2.0 × 0.6 m, with a thin film of epoxy (glue substance) and covering them with coarse sand or gravel of different sizes which have been previously segregated by sieving.

Five artificially roughened test beds are prepared for the experiments. Each bed has one size of the roughness elements. The roughness elements (gravel or coarse sand) are uniformly distributed as close to each other as possible on the top surface of the steel plate. Some of these test beds are shown in Figs. 4 and 5. Each of the roughened test beds is later fixed on the floor of the flume just downstream of the weir model. Fig. 6 shows general layout of the experiment.

Four different sizes of gravels and one size of coarse sand are used to study the effect of bed roughness on the properties of hydraulic jump. The gravel sizes are as follows: the first size retained on the 2 mm square mesh screen but passing the 4 mm square mesh screen, the second gravel size retained on the 4.00 mm square mesh screen but passing through the 4.75 mm square mesh screen, the third gravel size retained on 4.75 mm square mesh screen but passing through the 9.5 mm square mesh screen, and the fourth gravel size retained on the 12.5 mm square mesh screen but passing through the 19 mm square mesh screen. The coarse sand is retained on 1 mm square mesh screen but passing through the 2 mm square mesh screen.

6. Geometric Characteristics of Bed Roughness

6.1 Equivalent Heights of Rough Elements

The equivalent roughness height k_s, is defined by the height of the uniform thickness that will exist if all the rough elements on the test bed are imagined to be melted and spread uniformly over the steel plate. The equivalent heights of bed roughness used in this study are determined by dividing the water displaced volume of the roughness elements obtained using a graduated tank, over the area of the flat plate.

TABLE (2) EQUIVALENT HEIGHTS OF BED ROUGHNESS

ROUGH TEST BED	1-2mm	2-4mm	4-4.75mm	4.75-9.5mm	12.5-19mm
ks (mm)	0.46	1.15	2.64	4.83	8.29

ith the
ed with
al drop
iven in

for the
ting of
m, with
em with
ve been

ted for
oughness
nd) are
ible on
st beds
st beds
team of
of the

coarse
on the
are as
ze mesh
second
een but
e third
een but
e fourth
een but
rse sand
through

by the
all the
ted and
heights
ned by
elements
ne flat

.2.5-19mm
8.29

Fig. (4) Roughened Test Bed Composed of Course Sa
Passing Through The 2 mm Sieve and
Retained on The 1 mm Sieve.

Fig. (5) Roughened Test Bed Composed of Gravels
Passing Through The 19 mm Sieve and
Retained on The 12.5 mm Sieve.

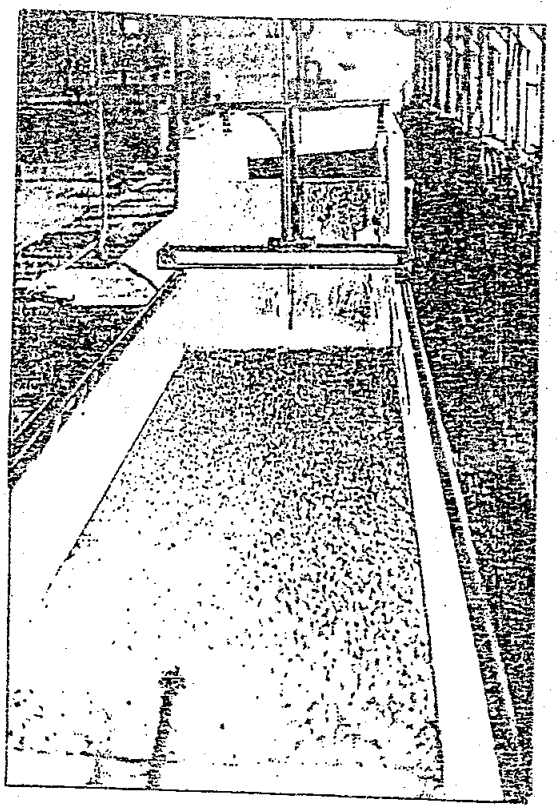

Fig. (6) General Layout of The Experiment.

6.2 Methods for Determining Roughness Height

There are different methods used for determining the height of the roughness elements. Some of these methods are described in the following:

(1) The Particle Height k_{65}

The roughness height k_{65} is defined as the particle size equal to or larger than 65% of the particles in the mixture. This roughness height was chosen by Huges and Flack [4]. In order to determine the roughness height k_{65} for the different rough beds of the present investigation, cross-sectional profiles of the rough bed are obtained by the lateral traversing of the test bed with the point gauge at some randomly chosen locations. The average values of the roughness height k_{65} calculated at the Various locations represent the entire rough bed, because of the uniform distribution of the gravel particles on the steel plate. The values of particle height distribution are summarized in Table 3.

TABLE (3) PARTICLE HEIGHT DISTRIBUTION

ROUGH TEST BED (mm)	PARTICLE HEIGHT IN (mm)		
	PERCENTILE		
	50	65	95
1-2	1.45	1.80	2.78
2-4	2.23	2.86	4.23
4-4.75	4.78	4.21	6.19
4.75-9.5	4.81	5.85	8.06
12.5-19.0	10.6	11.83	16.4

(2) Campbell Roughness Height (r.m.s.)

According to ref.[2] a practical method for ascertaining roughness magnitude is the root-mean-square (r.m.s.) of the projection of roughness elements perpendicular to a plane taken through the lowest depression in the area surveyed (the rough test bed). The values of r.m.s. for the different types of the rough test beds are calculated from the cross-sectional profiles at the chosen locations.

(3) Another Method for Determining a Measure for The Roughness Height:

Height is found in the Russian hydraulics literature. Vizgo [11] gives the roughness height by the parameter Δ as a roughness measure.

When $d_m \leq 4.5$ mm $\quad \Delta = d_m$ (7)

and for $d_m > 4.5$ mm $\quad \Delta = 0.8\, d_m$ (8)

where, d_m = mean diameter of the gravel mixture, which is given by

$$d_m = 0.5\,(d_{max} + d_{min}) \tag{9}$$

where,

d_{max} = the size of the mesh screen of the sieve which will permit the passing of all particles of the mixture, and

d_{min} = the size of the mesh screen of the sieve which retains all particles of the mixture.

The values of the measure of the roughness height obtained for the five types of roughnesses according to the above mentioned methods are given in table 4.

TABLE (4) VALUES OF ROUGHNESS HEIGHT MEASURE OBTAINED BY DIFFERENT METHODS

ROUGH TEST BED	k_{os}(mm)	r.m.s (mm)	Δ (mm)
1-2 mm	1.80	1.70	1.50
2-4 mm	2.86	2.60	3.00
4-4.75 mm	4.21	4.00	4.40
4.75-9.5 mm	5.85	5.50	5.70
12.5-19 mm	11.83	11.2	12.6

7. Determination of the Effective Bottom of Rough Channels

Various studies refs.[1,4,2,10] have suggested that when roughness elements are closely spaced, the depth of flow should be measured from the water surface to some reference level between the crests and the troughs of the roughness elements.

A detailed description of the depth-correction analysis is given in this study. There is no standard method for locating the effective bottom in a rough irregular channel.

The following methods are suggested by some investigators:

1) The effective bottom is a hypothetical plane at a distance $0.2k_{os}$ below the plane connecting the most prominent projections in the mixture. This method places the effective bottom quite near the top of the particle mixture and seems to work best with fine, relatively uniform roughnesses such as sand ref.[4],

2) The effective bottom is assumed to coincide with an alternative equivalent roughness height A_p/W_o, in which A_p = the cross-sectional are of the rough elements and W_o = the width of the working section. Fig. 7 shows the definition of these symbols. This method places the effective bottom well down in the particle voids and has been used with the larger sized gravel ref.[4]. The cross-sectional profiles are used to obtain the cross-sectional area of the rough elements A_p. The area under the profile is calculated using the trapezoidal rule.

3) The root-mean-square method is also used to determine the effective bottom for some investigations ref.[2], and

4) The parameter Δ obtained as a measure for the roughness height used in Russian hydraulic literature for the determination of the effective bottom departure ref.[11].

The results obtained by the different methods used for locating the effective bottom are summarized in table 5.

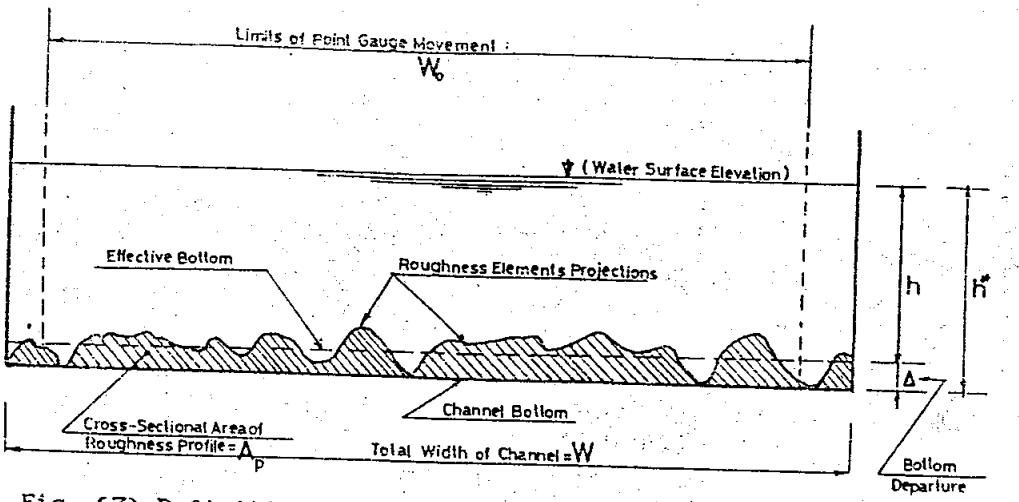

Fig. (7) Definition Sketch for The Cross-Sectional Profile of Roughness Elements.

TABLE (5) BOTTOM DEPARTURE FOR THE DIFFERENT TYPES OF ROUGH TEST BEDS.

ROUGH TEST BED	METHOD OF CALCULATION			
	dmax-0.2kσs (mm)	Ap/Wo (mm)	r.m.s. (mm)	Δ (mm)
1-2 mm	1.80	1.35	1.70	1.50
2-4 mm	2.86	2.00	2.60	3.00
4-4.75 mm	4.21	4.30	4.00	4.40
4.75-9.5 mm	5.85	4.55	5.50	5.70
12.5-19 mm	11.83	9.85	11.2	12.6

It is to be pointed out that the values of the bottom departures used in this study are the values of Δ. This is thought to be the simplest method in practice.

8. Experimental Results

The experiments are carried out using the different weir models described in section 4. Each of the six types of test beds is used with the four weirs of the present investigation. Six to nine different values of the rate of discharge in the range 5 < Q <20 lit/sec are used with each weir model with a discharge incremental increase ΔQ of about 2 lit/sec The total number of experimental runs is about 180 runs. Observations are repeated for each experimental run to record the following, the upstream depth of the hydraulic jump, the tailwater depth which represents the jump sequent depth, the length of the jump which is measured horizontally

from the upstream section of the jump to a point on the water surface where the downstream flow first becomes relatively uniform and the average flow depth reaches its maximum value (where the flow begins to be free from eddies), and the visual water surface profile of some of the occurring hydraulic jumps are also recorded.

The experimental range of the present measurements for each weir model determines the range of the flow dimensionless parameters, namely: the Froude number at the upstream section of the hydraulic jump, the conjugate depth ratio of the hydraulic jump and the Reynolds number at the upstream section of the hydraulic jump. Table 6 presents the respective range of the above mentioned parameters.

TABLE (6) EXPERIMENTAL RANGE OF THE DIMENSIONLESS FLOW PARAMETERS

WEIR DROP HEIGHT Z cm	UPSTREAM FROUDE NO. $F_1=U_1/\sqrt{gh_1}$	CONJUGATE DEPTH RATIO h_2/h_1	UPSTREAM REYNOLDS NO. $R_{e1}=4U_1h_1/\nu$
11	2.53 - 6.52	3.41 - 6.68	72852 - 46820
22.3	4.37 - 8.56	5.65 - 8.86	121442- 44918
32.5	5.14 - 10.91	7.38 - 10.6	130360- 48328
43	6.58 - 14.09	8.40 - 13.44	112459- 66229

9. Analysis and Discussion of the Results

The experimental results of the present investigation are graphically represented in this section. The results include the relationships between the rate of discharge and the length of the hydraulic jump and the tailwater depth over different types of test beds. The water surface profiles obtained for the hydraulic jumps formed over the various types of test beds are displayed for different flow conditions (different Froude numbers).

A useful empirical equation is deduced in the present experimental investigation to give the ratio of the length of the hydraulic jump formed on the rough bed to the respective length of the jump occurring on the smooth bed (L_j/L_s) as a function of the relative roughness Δ/h_2, where Δ is the measure of the roughness height and h_2 is the jump downstream water depth.

9.1 The Relationship between The Rate of Discharge and The Jump Length over The Different Types of Test Beds

Figs. 8, 10, 12, and 14 show the variations of the length of the hydraulic jump with the rate of discharges over the different types of test beds used with the four weir models. All figures display increasing jump length with the corresponding increase in the rate of discharge flowing over the same test bed.

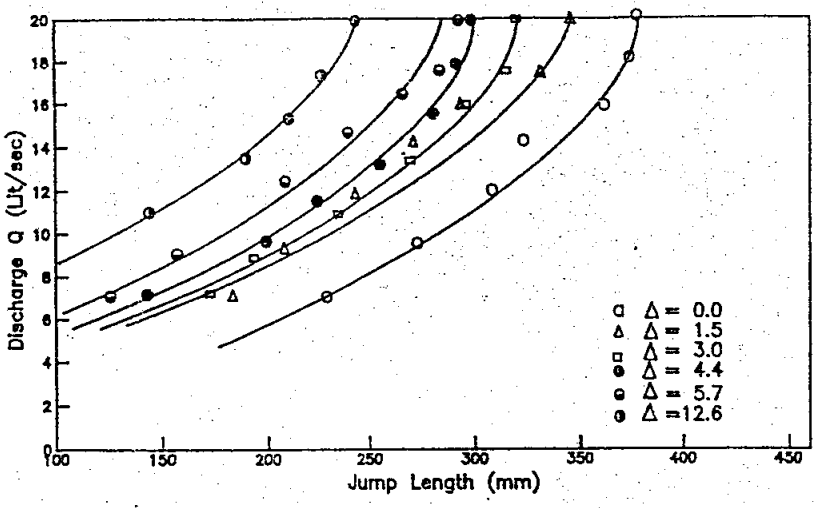

Fig. (8) Relationship between Discharge and Jump Length for Weir Model No. 1 Drop Height (Z = 11 cm)

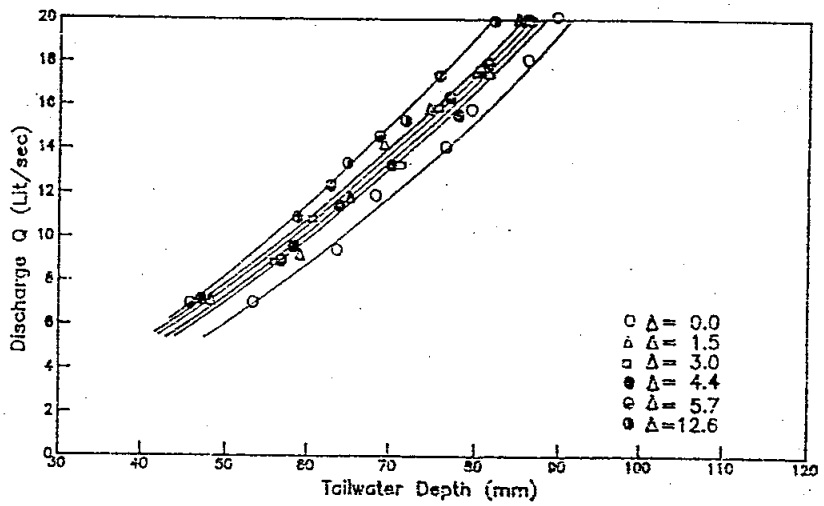

Fig. (9) Relationship between Discharge and Tailwater Depth for Weir Model No. 1 Drop Height (Z = 11 cm)

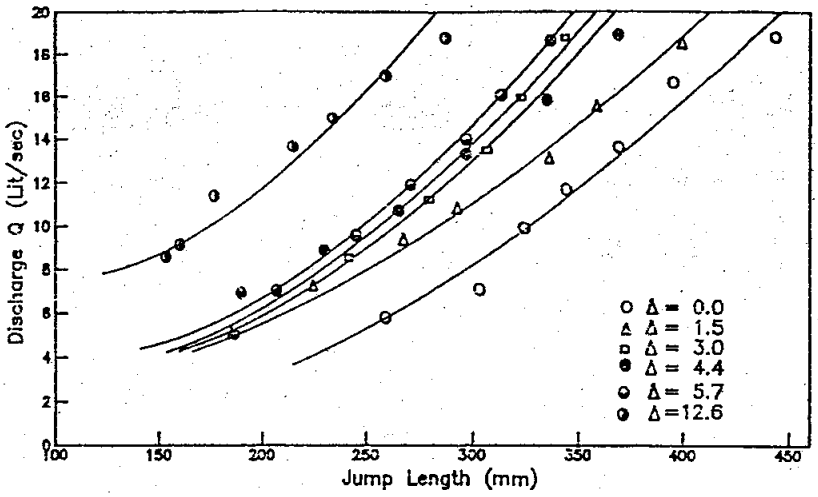

Fig. (10) Relationship between Discharge and Jump Length for Weir Model No. 2 Drop Height (Z = 22.3 cm)

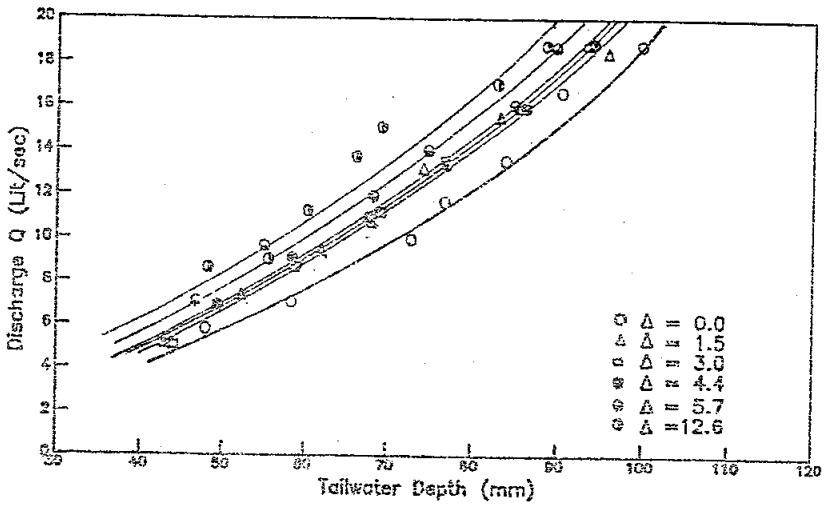

Fig. (11) Relationship between Discharge and Tailwater Depth for Weir Model No. 2 Drop Height (Z = 22.3 cm)

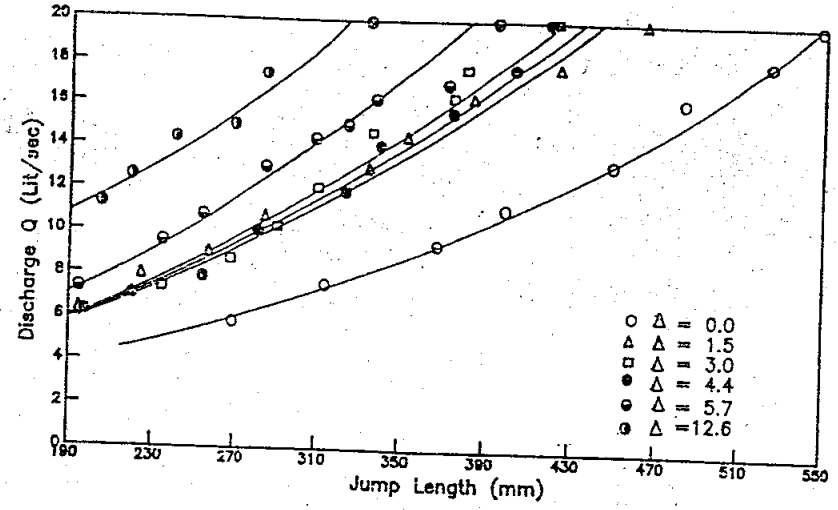

Fig. (12) Relationship between Discharge and Jump Length for Weir Model No. 3 Drop Height (Z = 32.5 cm)

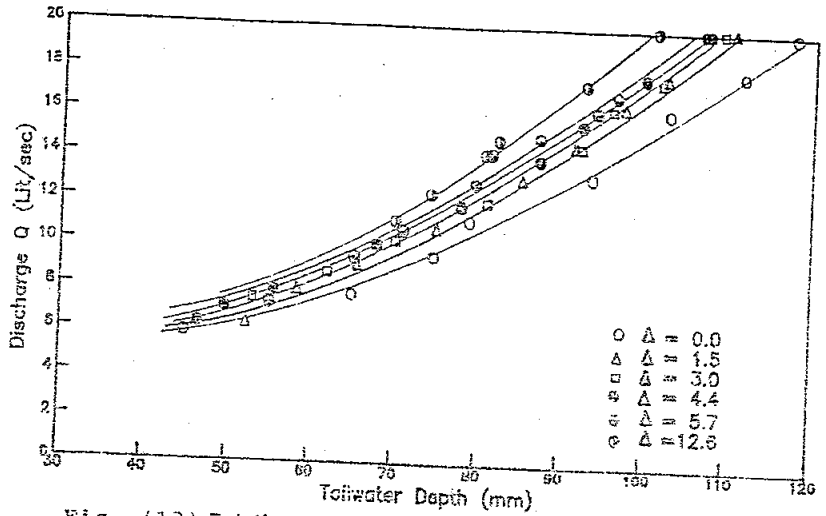

Fig. (13) Relationship between Discharge and Tailwater Depth for Weir Model No. 3 Drop Height (Z = 32.5 cm)

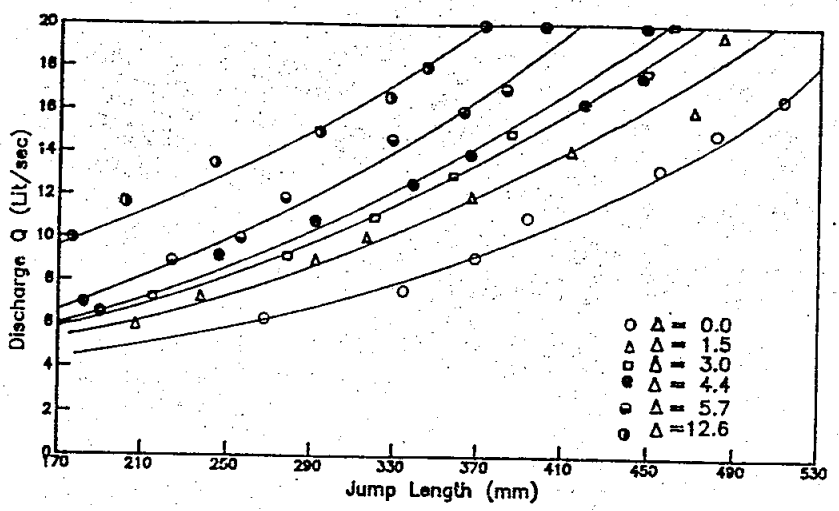

Fig. (14) Relationship between Discharge and Jump Length for Weir Model No. 4 Drop Height (Z = 43 cm)

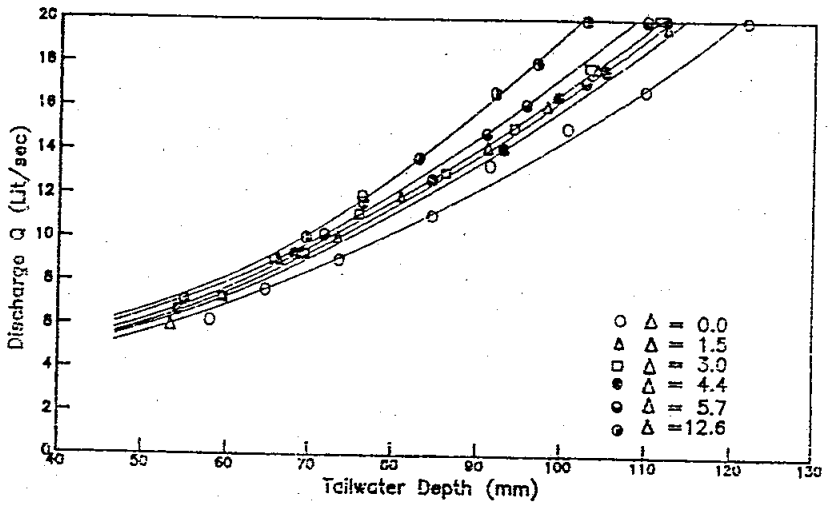

Fig. (15) Relationship between Discharge and Tailwater Depth for Weir Model No. 4 Drop Height (Z = 43 cm)

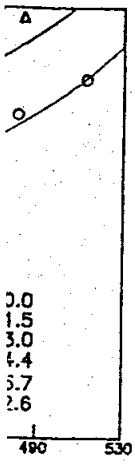

Weir Model No. 4

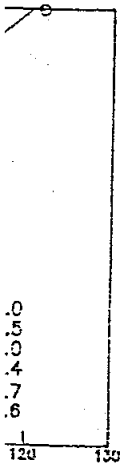

ter Depth
= 43 cm)

The figures show a general decrease in jump length wit the corresponding increase in bed roughness for a given valu of the rate of discharge. However, some overlap is observe between the experimental points for the test bed of Δ = 1.5 3 and 4.4 mm. This is due to the error incurred in estimati the jump length. Perhaps, this is expected because th downstream end of the jump cannot be located with a grea degree of precision, since the end of the jump does nc remain fixed but pulsates upstream and downstream. Therefor it is for the observer to visually average the pulsations o the jump end, which should result in a slight variations i determining the jump length. The figures also show that th length of the hydraulic jump occurring on the same test be increases with the corresponding increase in the drop height of the weir model.

9.2 The Relationship between The Rate of Discharge and The Tailwater Depth over The Different Types of Test Beds

Figs. 9, 11, 13, and 15 show the variations of tailwat depths with the rate of discharge over different types test beds used with the four weir models. The figures sho that over the same test bed the tailwater depth increase with the increasing of the rate of discharge. Also, decrease in the tailwater depth occurs for the same rate discharge when the bed roughness is increased. Some overla between the experimental results of the test beds with smal roughness height Δ = 1.5, 3 and 4.4 mm is observed. This because of the presence of some fluctuations in the level the tailwater depth. All figures also show increasin tailwater depth with the corresponding increase in the dro height of the weir model.

9.3 The Relationship between The Term (Lj/Ljo)h2 and The Absolute Roughness Height Δ

Some values of the rate of discharge were selected fro Figs. 10, 11, 14, and 15 between 10 and 20 Lit/Sec with a increment of 2 Lit/Sec. The corresponding values of Lj, L and h2 are obtained. Then the term (Lj/Ljo)h2 is computed fo different types of test beds and the relation betwe (Lj/Ljo)h2 and the absolute roughness height Δ is plotted fo the different rates of discharge and shown in Figs. 16 an 17. This relation shows a decrease in the term (Lj/Ljo)h with the increase in bed roughness for a given value the rat of discharge. Also, for the same bed roughness (same tes bed) the term (Lj/Ljo)h2 increases with the increasing of th discharge rate, as shown in Figs. 16 and 17.

9.4 The Ratio of Jump Length over a Rough Bed to Jump Lengt over a Smooth Bed as a Function of The Relative Roughne Height Δ/h2

A useful empirical equation is deduced from the presen experimental results to give the ratio of the jump lengt over a rough bed to the jump length over a smooth bed Lj/L as a function of the relative roughness height Δ/h2.

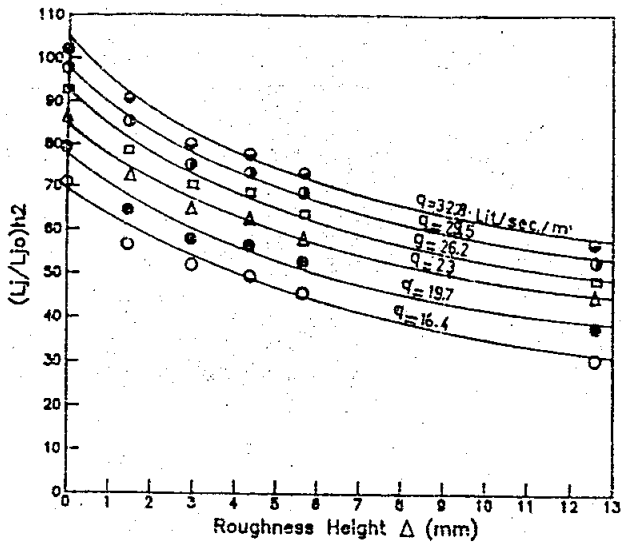

Fig. (16) Relationship between (Lj/Ljo)h2 and Absolute Roughness Height, Δ, for Weir Model No. 2

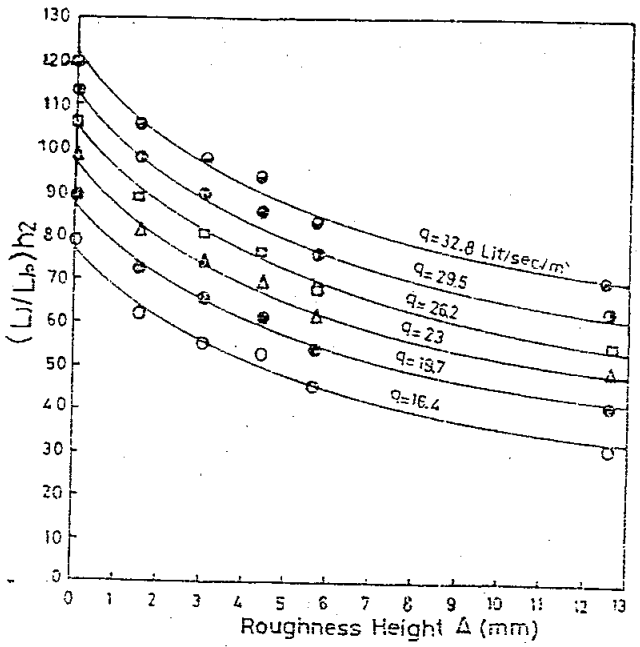

Fig. (17) Relationship between (Lj/Ljo)h2 and Absolute Roughness Height, Δ, for Weir Model No. 4

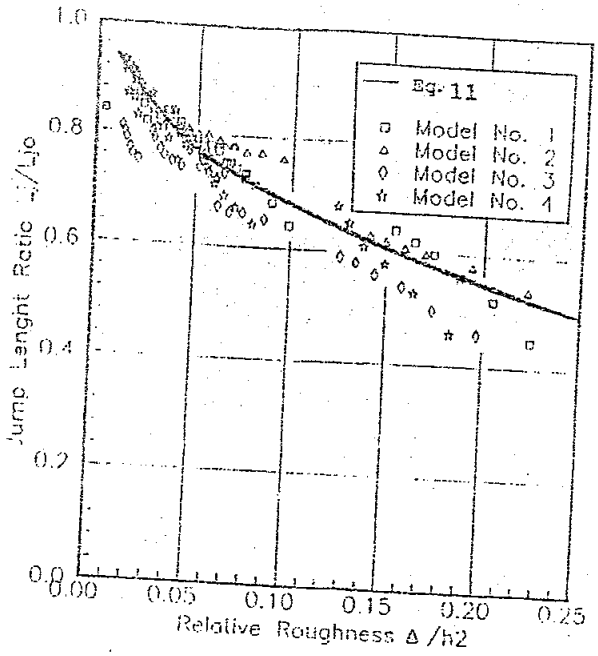

Fig.(18) Relation between Lj/Ljo and Δ/h2.

The ratio (Lj/Ljo) is plotted in Fig. 18 versus the relative roughness (Δ/h2). Then a best fit curve is obtained to represent the relation which is expressed in the form,

$$\frac{Lj}{Ljo} = 1 - 0.980399\left[\frac{\Delta}{h_2}\right]^{0.485264} \qquad (10)$$

The above relation (Eq. 10) may also be simplified in the form,

$$\frac{Lj}{Ljo} = 1 - \sqrt{\left[\frac{\Delta}{h_2}\right]} \qquad (11)$$

Also, it is seen that as the relative roughness increases, the ratio (Lj/Ljo) decreases. The ratio Lj/Ljo = 1.0 for the smooth bed case (Δ = 0) and equals 0.50 for the bed of a relative roughness height of 0.25. This shows that the reduction in the jump length is quite appreciable compared with the length of the jump over a smooth bed when the relative roughness is large.

The following table presents comparison of length ratio obtained from both relations for the different relative roughness Δ/h2. This proves that the above two relations are almost equivalent.

Δ/hz	Lj/Ljo	
	Eq.(11)	Least-Square Method, Eq.(10)
0	1	1
0.05	0.776	0.771
0.10	0.683	0.679
0.15	0.613	0.6095
0.20	0.553	0.551
0.25	0.500	0.49968

9.5 Results of Water Surface Profile

Figs. 19 to 24 show the typical water surface profiles over different types of test beds for number of experimental runs. The effective bottom for each test bed is shown in these figures. These figures also show that the shape of the free surface of the rough bed jumps is compacted compared with the smooth bed jumps and also this compactness increases with increasing of the bed roughness. This is consistent with the reduction in both parameter of the jump length and the jump conjugate depths over the rough bed.

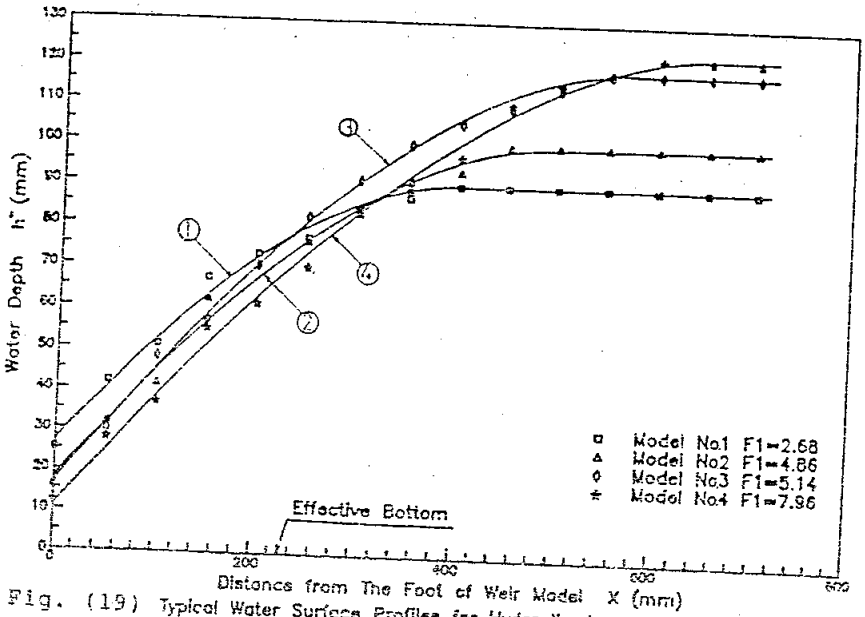

Fig. (19) Typical Water Surface Profiles for Hydraulic Jump over Smooth Bed

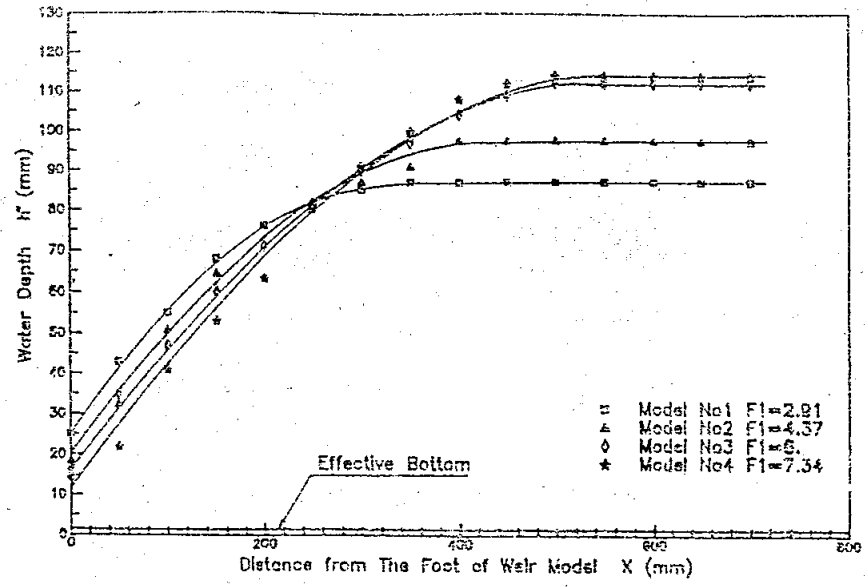

Fig. (20) Typical Water Surface Profiles for Hydraulic Jump over 1.0–2.0 mm Test Bed

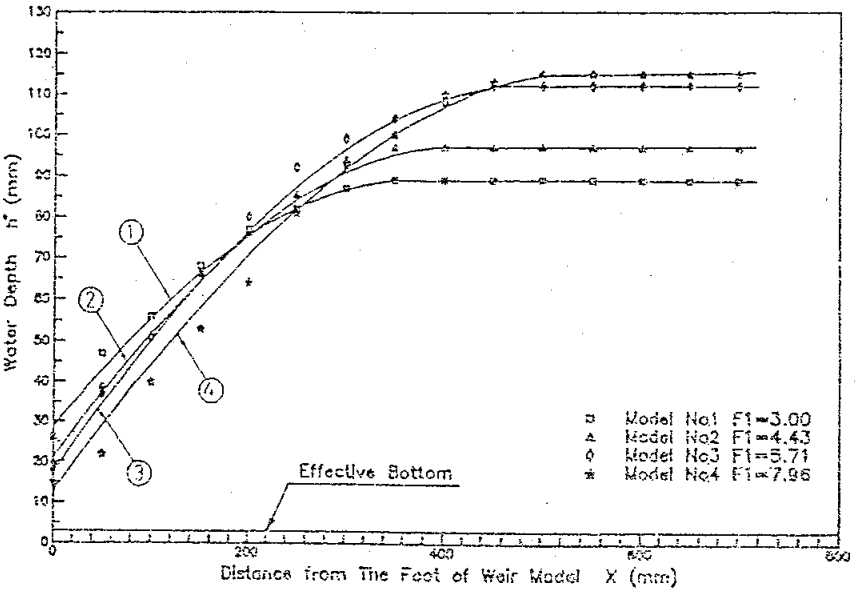

Fig. (21) Typical Water Surface Profiles for Hydraulic Jump over 2.0–4.0 mm Test Bed

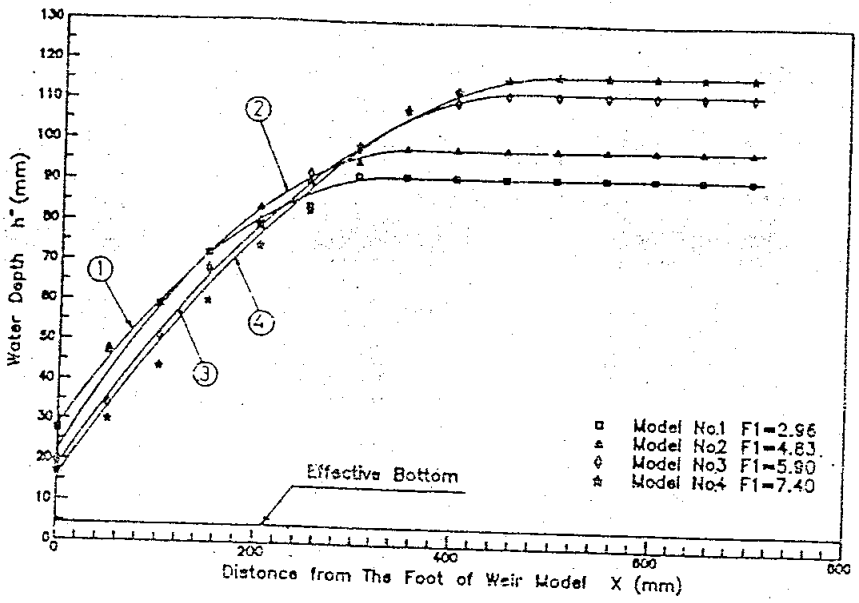

Fig. (22) Typical Water Surface Profiles for Hydraulic Jump over 4.0–4.75 mm Test Bed

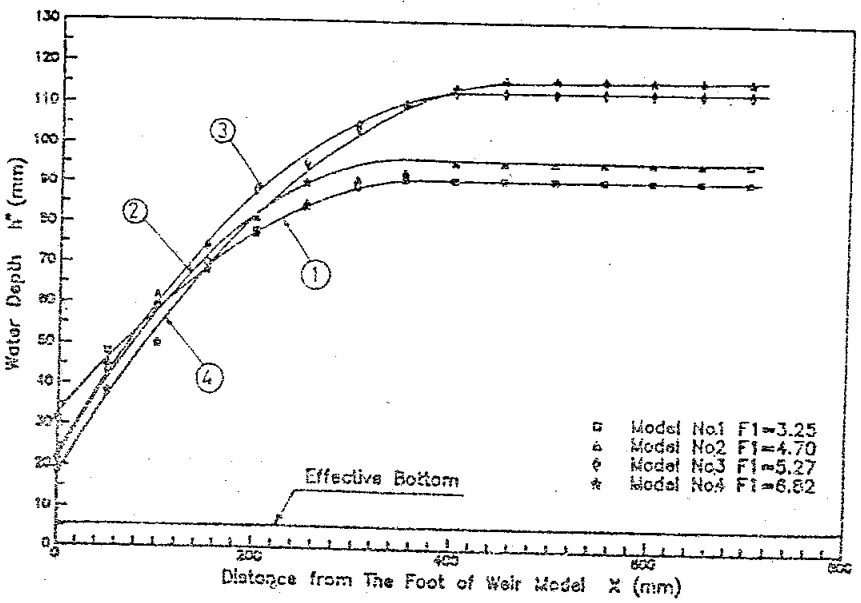

Fig. (23) Typical Water Surface Profiles for Hydraulic Jump over 4.75–9.5 mm Test Bed

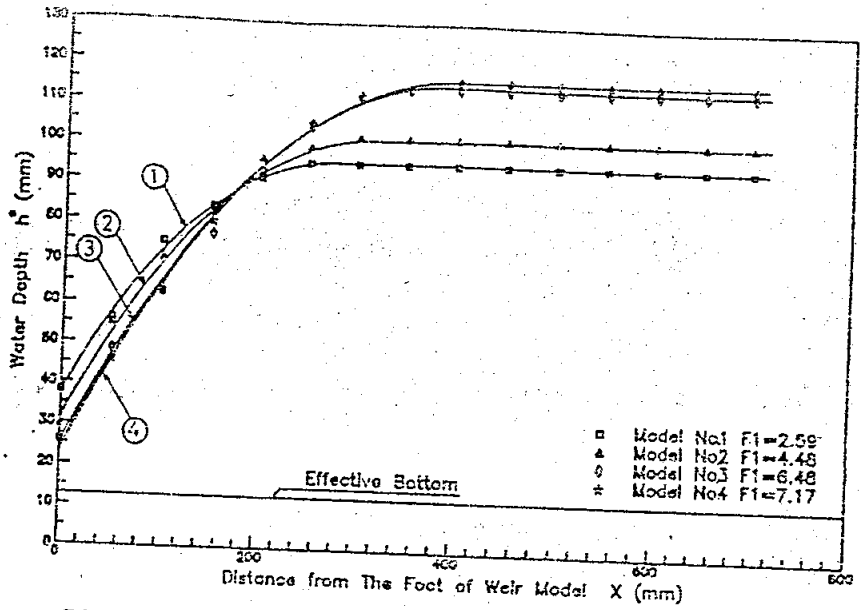

Fig. (24) Typical Water Surface Profiles for Hydraulic Jump over 12.5–19 mm Test Bed

7.1 Conclusions

This paper concerns the determination of the hydraulic jump properties over rough impervious beds. An extensive experimental study of the hydraulic jump occurring on smooth and rough test beds are carried out. The following conclusions are made:

The present experimental results of the hydraulic jump formed on a smooth bed showed good agreement with both of the respective experimental results by other investigators, and the results obtained from theoretical relationships for the classical hydraulic jump.

It was found that both the length of jump and the tailwater depth would vary with the supercritical Froude number and the relative roughness. The free surface profile of the rough bed jump is more compact when compared with respective hydraulic jump over the smooth bed. The experimental visual observations showed that the roughness reduces the amount of wave formation in the hydraulic jump.

A useful empirical equation has been deduced from the experimental results which describes the ratio of the jump length over a rough bed to the corresponding length over a smooth bed as a function of the relative roughness height, Δ/hz, (Eq. 11).

REFERENCES

1. Bathurst, J. C.; Li, R; and Simons, D. B., "Resistance Equation for Large-Scale Roughness", Journal of the Hydraulics Division, ASCE, Vol. 107, No. HY12, Proc. paper 16743, Dec., 1981, pp. 1593-1613.

2. Cassidy, J. J, and Bauer, W. J., Discussion of "Boundary layer Development and Spillway Energy Losses", by F. B. Campell, Journal of the Hydraulics Division, ASCE, No. HY2, pp. 370-378, March, 1966.

3. El-Feki, A. M., "Effect of the Bed Sand Roughness on the Geometry of the Hydraulic Jump", M. Sc. Thesis, University of El-Mansoura, March, 1990.

4. Hughes, W. C., and Flack, J. E., "Hydraulic Jump Properties over a Rough Bed", Journal of Hydraulic Engineering, Vol. 110, No. 12, Dec. 1984, ASCE, ISSN, paper No. 19347, pp. 1755-1772.

5. Leutheusser, H. J. and Kartha, V.C., "Effects of Inflow Condition on Hydraulic Jump", Journal of the Hydraulics Division, ASCE, Vol. 98, No. HY8, proc. paper 9088, Aug. 1972, pp. 1367-1385.

6. Leutheusser, H. J. and Schiller, E.J., "Hydraulic Jump in a Rough Channel", Water Power and Dam Construction, Vol. 27, No. 5, May, 1975, pp. 186-191.

7. Miller, P. A., "Behavior of the Rectangular Jump over a Rough Porous Bed", M. Sc. thesis, University of Colorado, 1984.

8. Oden, J. D., "Characteristics of the Hydraulic Jump over a Rough-Porous Bed", M. Sc. Thesis, University of Colorado, 1981.

9. Rajaratnam, N. and Subramanya, K., "Profile of the Hydraulic Jump", Journal of the Hydraulics Division, ASCE, Vol. 94, No. HY3, proc. paper 5931, May, 1968, pp. 663-673.

10. Rajaratnam, N., "Hydraulic Jumps on Rough Beds", Transactions of the Engineering Institute of Canada, Vol. 11, No. A-2, May, 1986. pp. 1-8.

11. Vizgo, M.C., Institute of Water Problems and Hydraulics, Academy of Scince, Technical Bulletin No. 12, Tashkent, 1963.

APPENDIX : NOTATIONS.

The following symbols are used in this paper,

Symbol	Definition
A_P	Area of the cross sectional profile of the gravel mixtures.
$d_{max.}$	The size of the mesh screen of the sieve which will permit the passing of all particles of the mixture.

$d_{min.}$	The size of the mesh screen of the sieve which retains all particles of the mixture.
d_m	Mean diameter of the gravel test bed.
$f_n(\ )$	An arbitrary function.
F_1	Supercritical Froude number, $U_1/\sqrt{gh_1}$.
g	Acceleration due to gravity.
H	Head over weir model, Fig. 1.
h_1	Effective depth of flow at the jump toe.
h_2	Effective depth of flow at the jump heel.
h_1'	Measured flow depth at the jump toe.
h_2'	Measured flow depth at the jump heel.
k_s	Equivalent sand grain roughness (Nikuradse).
k_s	Equivalent roughness height.
k_{s_m}	Measure of roughness size for gravel beds.
L_j	Length of jump, Fig. 1.
p	Height of weir model.
q	Discharge per unit width, Q/W.
W	Width of channel.
W_c	Width of the working section of the test bed, Fig. 7.
Z	Drop height of weir model.
Z_e	Effective drop height of weir model, (Z-Δ).
γ	Specific weight of water.
Δ	Effective height of roughness elements, Fig.7.
μ	Dynamic viscosity.
ν	Kinematic viscosity.
Π_n	Non-dimensional term, $(M^oL^oT^o)$.
ρ	Density.